© 2000 The Chemical Society of Japan

Bull. Chem. Soc. Jpn., 73, 85—95 (2000) 85

Behaviors of the One-Electron Reduction Species of $\{RuNO\}^6$-Type Complexes. An Oxygen-Transfer Reaction Occurs in the Nitrosyl Site of *cis*-$[Ru(NO^{\bullet})X(bpy)_2]^{n+}$ ($X = ONO_2$ for $n = 1$, $X = CH_3CN, H_2O$ for $n = 2$) ($\{RuNO\}^7$-Type) to Give an Identical Nitro Species[1]

Masao Mukaida,[*,†] **Yoshinobu Sato, Hideji Kato, Mami Mori, Dai Ooyama,**[††]
Hirotaka Nagao, and F. Scott Howell[*]

Department of Chemistry, Faculty of Science and Engineering, Sophia University,
Kioi-cho 7-1, Chiyoda-ku, Tokyo 102-8554

†Sophia School of Social Welfare, Kioi-cho 7-1, Chiyoda-ku, Tokyo 102-8554

††Department of Education, Fukushima University, Matsukawa 960-1296

(Received April 19, 1999)

Degradation sequences of *cis*-$[Ru(NO^{\bullet})X(bpy)_2]^{n+}$ ($X = ONO_2$, OCHO, OCOMe, NO_2, Cl for $n = 1$; $X = CH_3CN$, H_2O for $n = 2$) ($\{RuNO\}^7$-type), a one-electron reduction species of $\{RuNO\}^6$-type complexes, were investigated in CH_3CN by monitoring using electrochemical techniques (both cyclic and hydrodynamic voltammetries). The results show that an oxygen transfer occurs effectively at the nitrosyl site of *cis*-$[Ru(NO^{\bullet})X(bpy)_2]^{n+}$ ($X = ONO_2$ for $n = 1$, $X = CH_3CN$, H_2O for $n = 2$) to give identical nitro species, *cis*-$[Ru(NO_2)(CH_3CN)(bpy)_2]^+$. The extent that the nitrosyl-to-nitro conversion proceeded, however, differs depending on the X ligands; $X = CH_3CN$ and H_2O complexes gave the nitro species in almost 40% yield, while $X = ONO_2$ complex afforded nearly 80%. The monitoring results of the degradation sequences, along with the differences in yields, suggest that different processes are operating separately in the oxygen-transfer reaction. We propose some possible processes for both reactions, although a further investigation is needed for a detailed explanation.

The reaction of nitrosyl to give nitro is a key step in the biological nitrate–ammonia conversion.[2,3] The nitrosyl-to-nitro conversions reported so far proceed in principle by an acid–base reaction of the coordinated nitrosyl or a disproportination of nitrogen monoxide:[4—7]

$$M\text{–}NO^+ + 2OH^- \longrightarrow M\text{–}NO_2^- + H_2O \tag{1}$$

$$M\text{–}NO + 2NO \longrightarrow M\text{–}NO_2 + N_2O \tag{2}$$

Recently, an electrochemically-induced nitrosyl-to-nitro conversion which occurs accompanied by a two-electron reduction of $\{RuNO\}^6$-type nitrosyl complexes has been cited by Meyer et al.,[8,9] without any detailed investigation. A similar reaction was also found in our previous study of the one-electron reduction species of the $\{RuNO\}^6$-type complex, *cis*-$[Ru(NO^{\bullet})(CH_3CN)(bpy)_2]^{2+}$ ($\{RuNO\}^7$-type);[10] both of these reactions fall into different categories from those of Eqs. 1 and 2. As an extended study, we report here on the behavior of $\{RuNO\}^7$-type complexes (*cis*-$[Ru(NO^{\bullet})X(bpy)_2]^{n+}$ ($X = ONO_2$ for $n = 1$; $X = CH_3CN$, H_2O for $n = 2$)), in which an electrochemically-induced oxygen transfer can be found via a nitrosyl-to-nitro conversion reaction. A detailed study has shown that the conversion is initiated by the formation of *cis*-$[Ru(NO^{\bullet})(CH_3CN)(bpy)_2]^{2+}$ ($\{RuNO\}^7$), either in *cis*-$[Ru(NO^{\bullet})(ONO_2)(bpy)_2]^+$ ($\{RuNO\}^7$) or in *cis*-$[Ru(NO^{\bullet})(H_2O)(bpy)_2]^{2+}$ ($\{RuNO\}^7$). Interestingly, another conversion process, which differs from those of *cis*-$[Ru(NO^{\bullet})X(bpy)_2]^{2+}$ ($X = CH_3CN, H_2O$) ($\{RuNO\}^7$), proceeds in *cis*-$[Ru(NO^{\bullet})(ONO_2)(bpy)_2]^+$ ($\{RuNO\}^7$). A part of these results has been reported previously.[10]

Experimental

Materials. Bis(bipyridine) type ruthenium complexes with nitrosyl (*cis*-$[Ru(NO^+)X(bpy)_2]^{(n+1)+}$ (X = OCHO,[10] Cl,[11] ONO,[12] NO_2,[12] H_2O,[13] CH_3CN[13]) were prepared by reported procedures, using *cis*-$[Ru(NO_2)_2(bpy)_2]\cdot H_2O$. The dinitro complex was obtained by a reaction between a free NO_2^- and *cis*-$[RuCl_2(bpy)_2]Cl$.[14] Authentic samples used for the characterization of the degradation products of $\{RuNO\}^7$-type nitrosyl complexes (*cis*-$[Ru(NO_2)(CH_3CN)(bpy)_2](PF_6)$ and *cis*-$[Ru(CH_3CN)_2(bpy)_2](PF_6)_2$) were obtained by previously reported syntheses.[10] All other reagents, including ^{15}N-nitric acid (95% $H^{15}NO_3$), were obtained commercially and were used as supplied. ^{15}N-labelled nitrato complexes (*cis*-$[Ru(^{15}NO^+)(ONO_2)(bpy)_2](PF_6)_2$ and *cis*-$[Ru(NO^+)(O^{15}NO_2)(bpy)_2](PF_6)_2$) were prepared by the acid decompositions of *cis*-$[Ru(^{15}NO_2)_2(bpy)_2]$ and *cis*-$[Ru(NO_2)_2(bpy)_2]$ using HNO_3 and $H^{15}NO_3$, respectively.

Physical Measurements. Infrared spectra were recorded with a Perkin–Elmer FT-1650 spectrophotometer. Electrochemical measurements were performed in CH_3CN, under an argon stream with a supporting electrolyte, tetra-*n*-butylammonium hexafluorophosphate (TBAH) or tetraethylammonium perchlorate (TEAP), using a Huso polarograph Model 312; the current–potential waves were recorded with a Rikendenshi Instruments Model F-3F recorder. Three-electrode, one-compartment cells were used. They were equipped with a silver reference electrode (Ag|$AgNO_3$, 0.01 mol dm^{-3}). Controlled-potential electrolyses were performed in two-compartment cells using a platinum-gauze working electrode, with the auxiliary electrode in the second compartment separated by a glass frit. Hydrodynamic voltammograms (HDV) were performed using a rotating platinum working electrode with Nikko Keisoku Motor Speed Controller SC-5. The numbers of coulombs were measured by a Huso Model 343B digital coulometer.

Syntheses. ***cis*-[Ru(NO$^+$)(ONO$_2$)(bpy)$_2$](PF$_6$)$_2$·H$_2$O.** To a suspension of *cis*-$[Ru(NO_2)_2(bpy)_2]\cdot H_2O$ (50 mg/H_2O 10 cm^3) in a beaker was added concd HNO_3 (1 cm^3), and the solution was warmed on a hot plate at 80 °C for 3 h, during which time a cover glass was always used to prevent evaporation of the reaction solution (a portion of water was added to the solution during the warming procedure, to maintain the solution volume constant). In the final stage of the reaction, the solution volume was reduced to around 5 cm^3 by heating without a cover glass. The addition of NH_4PF_6 (solid) to the solution produced an orange-colored crystalline material, which was collected by filtration, washed with cold water, and then air-dried. Yield: 58 mg, 76%. A characterization of the product was established by the following data, along with the X-ray structure determination: Anal. Found: C, 29.73; H, 1.93; N, 10.46%. Calcd for $[Ru(NO^+)(ONO_2)(bpy)_2](PF_6)_2\cdot H_2O$: C, 29.53; H, 2.23; N, 10.33%. Diamagnetic property (Gouy method). Electrochemical property: $E_{1/2} = -0.06$, $E_{pc} = -0.77$ V. IR $\nu(NO^+$(nitrosyl)), 1941; $\nu_{as}(NO_2)$, 1522; $\nu_s(NO_2)$, 1263; ν(NO), 957 cm^{-1}. ^{13}C NMR (CD_3CN/TMS, ppm) δ = 155.91, 155.68, 154.87, 154.24, 154.21, 153.40, 151.96, 148.78, 145.67, 145.28, 144.65, 144.22, 130.65, 130.52, 130.18, 129.95, 127.05, 126.86, 126.61, 126.41. FAB-MS *m*/*z* 651 ($[Ru(NO)(NO_3)(bpy)_2](PF_6)$); 506 ($[Ru(NO)(NO_3)(bpy)_2]$).

***cis*-[Ru(NO$^+$)(OCOCH$_3$)(bpy)$_2$](ClO$_4$)$_2$·H$_2$O.** To an aqueous solution of *cis*-$[Ru(NO^+)(H_2O)(bpy)_2](ClO_4)_3\cdot 3H_2O$ (100 mg/10 cm^3) was added $CH_3COONa\cdot 3H_2O$ (167 mg), and then the solution pH was adjusted to 4 using a few drops of acetic acid. The solution was heated on a hot plate at 70 °C for 0.5 h with a cover glass, during which time the solution color changed from dark brown to bright orange. After the solution was cooled, $NaClO_4$ (50 mg) was added until a small amount of reddish-orange crystalline material was deposited. The solution was kept for one night in a refrigerator. The product was collected by filtration, washed with methanol and then ether, and air-dried. Anal. Found: C, 36.49; H, 2.94; N, 9.40%. Calcd for $[Ru(NO^+)(OCOCH_3)(bpy)_2](ClO_4)_2\cdot H_2O$: C, 36.73; H, 2.94; N, 9.73%. Yield: 82 mg, 95%.

***cis*-[Ru(NO$^+$)(OCOCH$_3$)(bpy)$_2$](PF$_6$)$_2$.** To an aqueous solution of *cis*-$[Ru(NO^+)(OCOCH_3)(bpy)_2](ClO_4)_2\cdot H_2O$ (100 mg/10 cm^3) was added NH_4PF_6 (30 mg) to give reddish-orange crystalline material. The product was collected by filtration, washed with methanol and then ether, and air-dried. Anal. Found: C, 33.25; H, 2.38; N, 8.82%. Calcd for $[Ru(NO^+)(OCOCH)(bpy)_2](PF_6)_2$: C, 33.35; H, 2.42; N, 8.84%. Yield: 99 mg, 88%.

Monitoring Study of the Degradation of $\{RuNO\}^7$-Type Complexes by the Measurements of Both Their Hydrodynamic Voltammograms (HDV) and Their Cyclic Voltammograms (CV). According to the previous technique,[12] a controlled potential reduction was carried out at −30 °C on *cis*-$[Ru(NO^+)X(bpy)_2]^{(n+1)+}$ ($\{RuNO\}^6$-type) complexes (1 mmol dm^{-3}) in CH_3CN at each reduction potential; the corresponding $\{RuNO\}^7$-type complexes were generated. After the electrolyses were finished, each electrolysis solution was allowed to stand at room temperature (20—23 °C) in order to elevate the solution temperature. Monitorings by both HDV and CV were carried out for the solutions over 24 h at regular intervals of the standing times. The variations in *I*d of both original $\{RuNO\}^7$-type complex and degradation products were estimated directly from the HDV graphically.

X-Ray Crystallographic Data Collection and Refinement of the Structure. Single crystals of $[Ru(NO^+)(ONO_2)(bpy)_2](ClO_4)_2\cdot H_2O$ were obtained by recrystallization from CH_3CN/Et_2O. A single crystal was mounted on a glass fiber. The crystallographic data are summarized in Table 1. The data were collected by the ω–2θ scan technique ($2\theta < 50°$) on a Rigaku AFC5S automated four-circle X-ray diffractometer with graphite-monochromatized Mo*Kα* radiation (0.71069 Å) at 23 °C. The cell constants were determined by least-squares fits to the setting parameters of 25 independent reflections. All of the calculations were carried out on an IRIS Indy computer of Silicon Graphic Corporation using the TEXSAN crystallographic software package of Molecular Structure Corporation. The structure of *cis*-$[Ru(NO^+)(ONO_2)(bpy)_2](ClO_4)_2\cdot H_2O$ was solved by a Patterson method and expanded using Fourier techniques. Empirical absorption corrections using Lorentz polarization and absorption were applied. The structure was refined by full-matrix least-square techniques. The non-hydrogen atoms were refined anisotropically. Hydrogen atoms were placed in idealized positions and included in structure-factor calculations. The final cycle of the full-matrix least-squares refinements was based on 3206 observations ($I > 3.00\sigma(I)$) and 379 variable parameters.

Table 1. Crystallographic Data of *cis*-$[Ru(NO)(ONO_2)(bpy)_2](ClO_4)_2\cdot H_2O$

Formula	$C_{20}H_{18}N_6O_{13}Cl_2Ru$
Fw	722.37
Crystal system	Monoclinic
Space group	$P2_1/n$
a/Å	8.757(2)
b/Å	14.553(2)
c/Å	20.100(2)
β/°	94.03(1)
V/Å^3	2555.2(8)
Z	4
Scan method	ω–2θ
Scan speed/deg min^{-1}	5
T/°C	20
D_{calcd}/g cm^{-1}	1.87
μ(Mo $K\alpha$)/cm^{-1}	9.04
Trans. factor	0.94—0.99
$2\theta_{max}$/deg	50.0
No. of unique data	4701
No. of observed data ($I > 3.00\sigma(I)$)	3206
No. of variables	379
R[a)]	0.036
R_w[b)]	0.028
Goodness of Fit Indicator	1.90

a) $R = \Sigma||F_o| - |F_c||/\Sigma|F_o|$.
b) $R_w = [\Sigma w(|F_o| - |F_c|)^2/\Sigma w|F_o|^2]^{1/2}$.

Crystallographic data have been deposited at the CCDC, 12 Union Road, Cambridge CB2 1EZ, UK and copies can be obtained on request, free of charge, by quoting the publication citation and the deposition number CCDC 136239. The lists of complete information on collected data and refinement, positional parameters and B_{eq}, anisotropic displacement parameters, and bond distances are deposited as Document No. 73009 at the Office of the Editor of Bull. Chem. Soc. Jpn.

Results

Synthesis and the Structure Determination of *cis*-$[Ru(NO^+)(ONO_2)(bpy)_2]^{2+}$ ($\{RuNO\}^6$). The complex *cis*-$[Ru(NO^+)(ONO_2)(bpy)_2]^{2+}$ was prepared newly as the most suitable compound for our present purpose. An IR absorption band due to a nitrosyl (ν(NO)) was found at 1941 cm^{-1}, which shifted to 1903 cm^{-1} in *cis*-$[Ru(^{15}NO^+)(ONO_2)(bpy)_2]^{2+}$. IR data are also consistent with a complex having NO_3^- through a single nitrate oxygen (see Experimental Section).[15] The bonding mode of the NO_3^- ligand was confirmed by an X-ray structure determination (Fig. 1 and Table 2). The coordination geometry of the cation has an octahedral arrangement with a linear Ru–NO group (178.0(4)°) *cis* to the nitrato ligand. The nitrosyl bond lengths of Ru–N and N–O are comparable to those in other linear nitrosyls. The structural parameters of the $\{Ru(NO)(bpy)_2\}$ moiety are also basically the same as those of *cis*-$[Ru(NO^+)X(bpy)_2]^{2+}$ (X = OCHO,[10] NO_2,[12] ONO,[12] Cl,[16]) reported recently. Other $\{RuNO\}^6$-type complexes, *cis*-$[Ru(NO^+)X(bpy)_2]^{(n+1)+}$ (X = H_2O, CH_3CN, OCHO), have been prepared and characterized,[10,12] while *cis*-$[Ru(NO^+)(OCOCH_3)(bpy)_2]^{2+}$ was obtained by modifying the procedures used to obtain *cis*-$[Ru(NO^+)(OCHO)(bpy)_2]^{2+}$.[10]

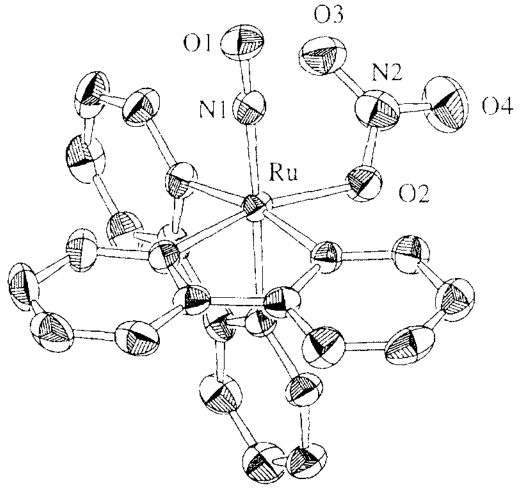

Fig. 1. ORTEP drawing of $[Ru(NO)(ONO_2)(bpy)_2](ClO_4)_2$.

Table 2. Selected Bond Lengths (Å) and Angles (°)

Ru–N1	1.747(4)
N1–O1	1.134(4)
N2–O2	1.332(5)
N2–O3	1.232(5)
N2–O4	1.222(5)
Ru–N1–O1	178.0(4)
O2–N2–O3	118.9(4)
O2–N2–O4	115.9(5)
O3–N2–O4	125.3(5)

The $\{RuNO\}^7$-Type Complexes Classified Based on Their Degradation Sequences. A monitoring study of the degradation processes of the $\{RuNO\}^7$-type complexes was attempted; such a monitoring study would enable us to evaluate the chemical reactions which occur accompanied by the degradation of the one-electron reduction species of the $\{RuNO\}^6$-type complexes. We obtained the $\{RuNO\}^7$-type complexes by an exhaust reductive electrolysis of the corresponding $\{RuNO\}^6$-type complexes in CH_3CN at −30 °C (a low temperature was adopted so as to avoid the initiation of any degradation reaction of the chemically unstable $\{RuNO\}^7$-type complexes during the electrolyses). The degradation patterns (described later) allowed us to classify the $\{RuNO\}^7$-type complexes into three groups: An oxygen transfer reaction occurred in the nitrosyl site of *cis*-$[Ru(NO^{\bullet})X(bpy)_2]^{n+}$ (X = ONO_2, CH_3CN, H_2O) to give *cis*-$[Ru(NO_2)(CH_3CN)(bpy)_2]^+$ in appreciable amounts (pattern **i**). Monitoring experiments showed that the existence of *cis*-$[Ru(NO^{\bullet})(CH_3CN)(bpy)_2]^{2+}$ is essential, as a precursor, for the oxygen-transfer reaction. The pattern **i** complexes can be further divided into two groups: X = CH_3CN, H_2O (pattern **i-a**) and X = ONO_2 (pattern **i-b**), based mainly on the degradation sequences. Such an oxygen-transfer reaction did not occur in *cis*-$[Ru(NO^{\bullet})Cl(bpy)_2]^+$ at all (pattern **ii**); an elimination of the nitrosyl moiety occurs in the pattern **ii** complex, without the formation of a precursor species (*cis*-$[Ru(NO^{\bullet})(CH_3CN)(bpy)_2]^{2+}$). Either the degradation observed in pattern **i** or that of **ii** occurred in the pattern **iii** complexes, *cis*-$[Ru(NO^{\bullet})X(bpy)_2]^+$ (X = OCOR (R = H, CH_3), NO_2), although the pattern **i** type degradation proceeded rather dominantly. The results are summarized in Scheme 1 and in Table 3.

Degradation Sequences of the $\{RuNO\}^7$-Type Complexes. *cis*-$[Ru(NO^{\bullet})(ONO_2)(bpy)_2]^+$. The cyclic voltammogram of *cis*-$[Ru(NO^+)(ONO_2)(bpy)_2](PF_6)_2$, measured at 20 °C in CH_3CN with 0.1 M $(Bu)_4NPF_6$ as a supporting electrolyte (1 M = 1 mol dm^{-3}), is shown in Fig. 2. The electron-transfer process of the first reduction wave (−0.10 V) is diffusion-controlled with $ip/v^{1/2}$ constant over the scan rate range used; the one-electron redox system is indicated by an analysis of the normal pulse voltammogram. The ratio of the cathodic-to-anodic peak current for the first wave ($[Ru(NO^+)(ONO_2)(bpy)_2]^{2+/+}$ couple) was nearly unity. Another irreversible wave appeared at a more negative potential region, −0.77 V. An exhaust reductive electrolysis carried out at 25 °C for the first reduction wave (−0.06 V) showed that the one-electron reduction of *cis*-$[Ru(NO^+)(ONO_2)(bpy)_2]^{2+}$ was followed by a rapid degradation to give *cis*-$[Ru(NO^{\bullet})(CH_3CN)(bpy)_2]^{2+}$. The generation of *cis*-$[Ru(NO^{\bullet})(CH_3CN)(bpy)_2]^{2+}$ could be confirmed by data from an authentic sample. Relatively small redox waves also appeared at more positive potential regions when the electrolysis progressed. The two waves observed at 0.81 and 1.10 V

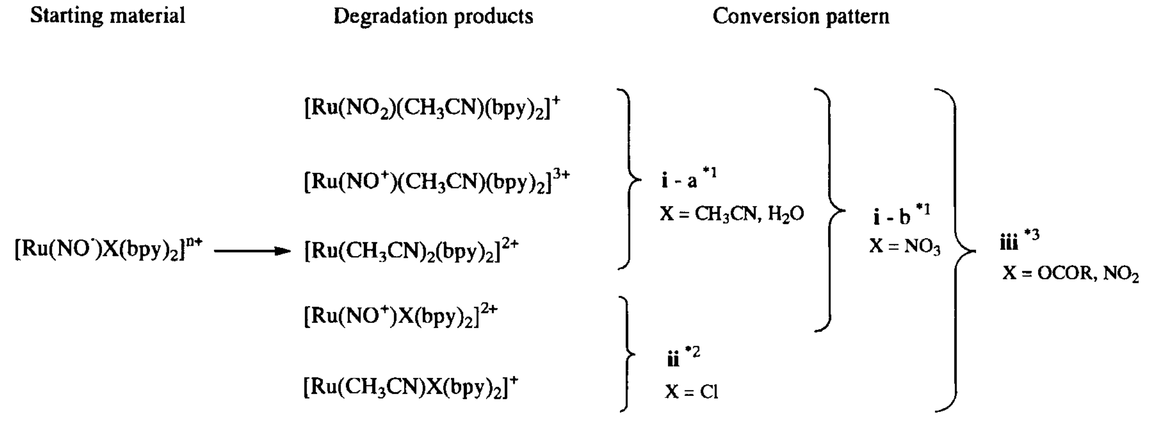

*1: Conversion process is not the same for **i-a** and for **i-b**.

*2: Only two species were generated without the formation of nitro species.

*3: Either the **i-a** or **ii** is operating.

Scheme 1. Schematic explanation for the conversion reactions of *cis*-$[Ru(NO^{\bullet})X(bpy)_2]^{n+}$.

Table 3. Degradation products of *cis*-$[Ru(NO^{\bullet})X(bpy)_2]^{n+}$ ($\{RuNO\}^7$)

X	Final main products	Other species[b)]	Degradation pattern
CH_3CN H_2O	$[Ru(NO_2)(CH_3CN)(bpy)_2]^+$ (35—40%)[a)] $[Ru(NO^+)(CH_3CN)(bpy)_2]^{3+}$ $[Ru(CH_3CN)_2(bpy)_2]^{2+}$		**i-a**
ONO_2	$[Ru(NO_2)(CH_3CN)(bpy)_2]^+$ (75—78 %)[a)] $[Ru(NO^+)(CH_3CN)(bpy)_2]^{3+}$ $[Ru(CH_3CN)_2(bpy)_2]^{2+}$ $[Ru(NO^+)(ONO_2)(bpy)_2]^{2+}$	$[Ru(NO^{\bullet})(CH_3CN)(bpy)_2]^{2+}$	**i-b**
Cl	$[Ru(NO^+)Cl(bpy)_2]^{2+}$ $[RuCl(CH_3CN)(bpy)_2]^+$		**ii**
HCOO CH_3COO NO_2	$[Ru(NO_2)(CH_3CN)(bpy)_2]^+$ (ca. 5%)[a)] $[Ru(NO^{\bullet})(CH_3CN)(bpy)_2]^{2+}$ $[Ru(CH_3CN)_2(bpy)_2]^{2+}$ $[Ru(NO^+)X(bpy)_2]^{2+}$ $[RuX(CH_3CN)(bpy)_2]^+$	c)	**iii**

a) (Figures in parentheses): yield of the nitro species. $([[Ru(NO_2)(CH_3CN)(bpy)_2]^+]/[[Ru(NO^{\bullet})X(bpy)_2]^{n+}])\times 100$. b) The species could be detected prior to the formation of final main products. c) The species could not be clarified owing to complexity of HDV (CV).

could be ascribed to *cis*-$[Ru(NO_2)(CH_3CN)(bpy)_2]^+$ and *cis*-$[Ru(CH_3CN)_2(bpy)_2]^{2+}$, respectively, again using authentic samples.

Since the above electrode-chemical reaction (E-C) was depressed in a low-temperature experiment (−30 °C), the degradation process of *cis*-$[Ru(NO^{\bullet})(ONO_2)(bpy)_2]^+$ ($\{RuNO\}^7$) could be monitored at 20 °C by hydrodynamic voltammograms (HDV); we first accumulated the one-electron reduction species by completing an exhaust reductive electrolysis of *cis*-$[Ru(NO^+)(ONO_2)(bpy)_2]^{2+}$ at −30 °C; a solution containing the resultant species, *cis*-$[Ru(NO^{\bullet})(ONO_2)(bpy)_2]^+$, was then warmed to 20—25 °C by standing the solution at room temperature under an argon stream. We found that the wave of *cis*-$[Ru(NO^{\bullet})(ONO_2)(bpy)_2]^+$ decreased rapidly, while that of *cis*-$[Ru(NO^{\bullet})(CH_3CN)(bpy)_2]^{2+}$ ($\{RuNO\}^7$) appeared and then it increased. When the solvation had progressed further, another chemical change occurred suddenly to give *cis*-$[Ru(NO_2)(CH_3CN)(bpy)_2]^+$, along with *cis*-$[Ru(CH_3CN)_2(bpy)_2]^{2+}$; this change terminated within about 2 h. During these 2 h the wave of *cis*-$[Ru(NO^{\bullet})(CH_3CN)(bpy)_2]^{2+}$ ($\{RuNO\}^7$) decreased. Noticeably, the wave of the original *cis*-$[Ru(NO^+)(ONO_2)(bpy)_2]^{2+}$ ($\{RuNO\}^6$) was generated during progress of the nitrosyl-to-nitro conversion, even though the experiment was carried out under an argon atmosphere in the dark. The results are shown in Fig. 3A and are summarized graphically in Fig. 3B.

***cis*-$[Ru(NO^{\bullet})(CH_3CN)(bpy)_2]^{2+}$ and *cis*-$[Ru(NO^{\bullet})(H_2O)(bpy)_2]^{2+}$.** Although the corresponding $\{RuNO\}^6$-type complexes have been investigated widely, the experi-

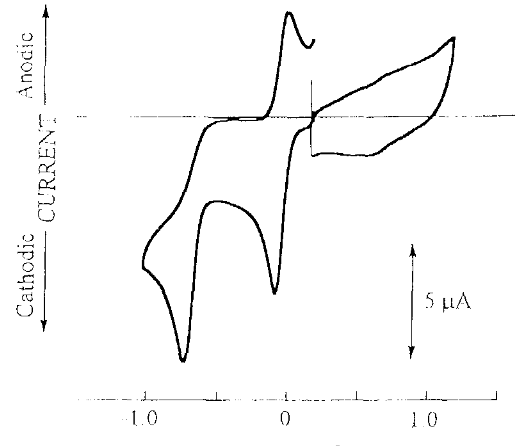

Fig. 2. Typical cyclic voltammogram of *cis*-[Ru(NO$^{\bullet}$)(ONO$_2$)(bpy)$_2$]$^+$ ({RuNO}^{7}).

mental results described here for the {RuNO}^{7}-type complexes have not yet been reported. The complex *cis*-[Ru(NO$^+$)(CH$_3$CN)(bpy)$_2$]$^{3+}$ showed a typical CV pattern as the {RuNO}^{6}-type complex.[17] Similar to the experiment carried out on *cis*-[Ru(NO$^{\bullet}$)(ONO$_2$)(bpy)$_2$]$^+$, a monitoring experiment was attempted for the electrochemically generated one-electron reduction species *cis*-[Ru(NO$^{\bullet}$)(CH$_3$CN)(bpy)$_2$]$^{2+}$ by both a hydrodynamic voltammogram (HDV) and CV. In contrast to the case of *cis*-[Ru(NO$^{\bullet}$)(ONO$_2$)(bpy)$_2$]$^+$, the generations of both *cis*-[Ru(NO$_2$)(CH$_3$CN)(bpy)$_2$]$^+$ and *cis*-[Ru(CH$_3$CN)$_2$(bpy)$_2$]$^{2+}$ are very slow (it took one night), and their product amounts were relatively low. The conversion ratio ([*I*d of the nitro species]/[*I*d of the original nitrosyl species]×100), estimated at the final reaction stage of the conversion reaction (30 h later), was only 35—40%. The original {RuNO}^{6}-type nitrosyl complex *cis*-[Ru(NO$^+$)(CH$_3$CN)(bpy)$_2$]$^{3+}$ was re-generated again during the progress of nitro complex formation. The results are shown in Fig. 4A and are summarized graphically in Fig. 4B. Essentially the same monitoring result has been observed in *cis*-[Ru(NO$^{\bullet}$)(H$_2$O)(bpy)$_2$]$^{2+}$, since the species changed easily to *cis*-[Ru(NO$^{\bullet}$)(CH$_3$CN)(bpy)$_2$]$^{2+}$ under the experimental conditions.[10,18]

***cis*-[Ru(NO$^{\bullet}$)Cl(bpy)$_2$]$^+$.** Similar to *cis*-[Ru(NO$^{\bullet}$)X(bpy)$_2$]$^{n+}$ ($n = 1$ for X = ONO$_2$ and $n = 2$ for both H$_2$O and CH$_3$CN) described above, *cis*-[Ru(NO$^{\bullet}$)Cl(bpy)$_2$]$^+$ belongs to the typical one-electron reduction species of {RuNO}^{6}-type complexes. However, the sequence of the degradation reaction of *cis*-[Ru(NO$^{\bullet}$)Cl(bpy)$_2$]$^+$ markedly differs. The monitoring experiment indicated that no *cis*-[Ru(NO$^{\bullet}$)(CH$_3$CN)(bpy)$_2$]$^{2+}$ was generated at all. Instead, both *cis*-[Ru(NO$^+$)Cl(bpy)$_2$]$^{2+}$ and *cis*-[RuCl(CH$_3$CN)(bpy)$_2$]$^{1+}$ appeared, and then increased at the expense of *cis*-[Ru(NO$^{\bullet}$)Cl(bpy)$_2$]$^+$, without the formation of *cis*-[Ru(NO$_2$)(CH$_3$CN)(bpy)$_2$]$^+$. Re-generation of the original {RuNO}^{6}-type complex (*cis*-[Ru(NO$^+$)Cl(bpy)$_2$]$^{2+}$) was found in appreciable amounts. The results are shown in Fig. 5A and are summarized graphically in Fig. 5B.

***cis*-[Ru(NO$^{\bullet}$)X(bpy)$_2$]$^+$ (X = OCHO, OCOCH$_3$).** Figures 6A and 6B show that, at a glance, the degradation patterns of *cis*-[Ru(NO$^{\bullet}$)X(bpy)$_2$]$^+$ (X = OCHO, OCOCH$_3$) appear to be very similar to those of *cis*-[Ru(NO$^{\bullet}$)X(bpy)$_2$]$^{2+}$ (X = H$_2$O, CH$_3$CN) (pattern **i-b**). However, the following differences are found; in addition to small amounts of the pattern **i-a** type products (*cis*-[Ru(NO$_2$)(CH$_3$CN)(bpy)$_2$]$^+$, *cis*-[Ru(CH$_3$CN)$_2$(bpy)$_2$]$^{2+}$, and *cis*-[Ru(NO$^+$)(CH$_3$CN)(bpy)$_2$]$^{3+}$), the pattern **ii** type products (*cis*-[RuX(CH$_3$CN)(bpy)$_2$]$^+$ and *cis*-[Ru(NO$^+$)X(bpy)$_2$]$^{2+}$ (X = OCHO,

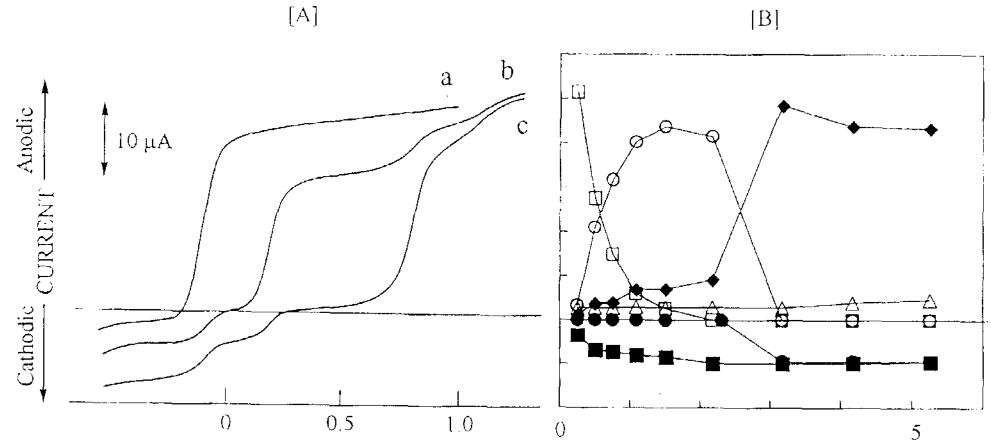

Fig. 3. The conversion process of *cis*-[Ru(NO$^{\bullet}$)(ONO$_2$)(bpy)$_2$]$^+$ ({RuNO}^{7}) monitored by hydrodynamic voltammograms (HDV) at 20 °C. [A] Monitoring results. a, Just after the electrolysis was completed (The measurement was carried out after the solution temperature was elevated from −30 to 20 °C); b, 2 h after allowing the electrolyzed solution to stand (*cis*-[Ru(NO$^{\bullet}$)(CH$_3$CN)(bpy)$_2$]$^{2+}$ was formed and then it increased); c, 4 h after the standing started (The formation of *cis*-[Ru(NO$_2$)(CH$_3$CN)(bpy)$_2$]$^+$ completed). [B] Plots of the standing times vs. *I*d values of the product species, each of which was estimated from the corresponding *I*d value of HDV. □ *cis*-[Ru(NO$^{\bullet}$)(ONO$_2$)(bpy)$_2$]$^+$ (−0.06 V), △ *cis*-[Ru(CH$_3$CN)$_2$(bpy)$_2$]$^{2+}$ (1.10 V), ■ *cis*-[Ru(NO$^+$)(ONO$_2$)(bpy)$_2$]$^{2+}$ ({RuNO}^{6}), ● *cis*-[Ru(NO)(CH$_3$CN)(bpy)$_2$]$^{3+}$ ({RuNO}^{6}) (0.19 V), ○ *cis*-[Ru(NO$^{\bullet}$)(CH$_3$CN)(bpy)$_2$]$^{2+}$ (0.19 V), ◆ *cis*-[Ru(NO$_2$)(CH$_3$CN)(bpy)$_2$]$^+$ (0.81 V).

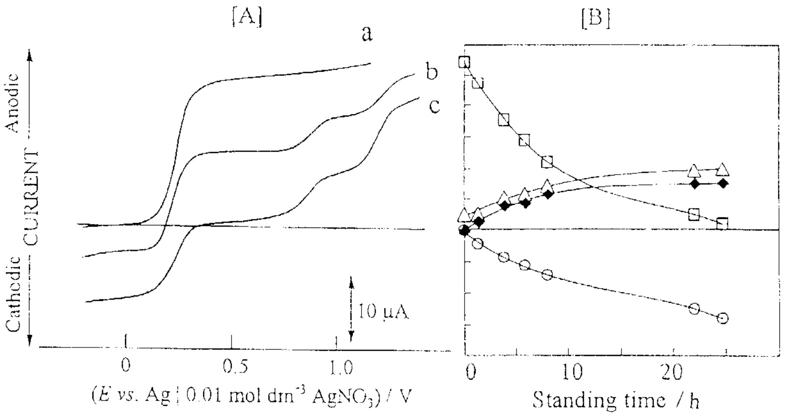

Fig. 4. The conversion process of *cis*-$[\mathrm{Ru(NO^{\bullet})(CH_3CN)(bpy)_2}]^+$ ($\{\mathrm{RuNO}\}^7$) monitored by hydrodynamic voltammograms (HDV) measured at 20 °C. [A] Monitoring results. a, Just after the electrolysis was completed (The measurement was carried out after the solution temperature was elevated from −30 to 20 °C); b, 5 h after beginning the standing (The three species described below were formed and they increased); c, after 22 h of standing. [B] Plots of standing times vs. *I*d values of the product species, each of which was estimated from the corresponding *I*d value of HDV. □ $[\mathrm{Ru(NO^{\bullet})(CH_3CN)(bpy)_2}]^{2+}$ (0.19 V), △ $[\mathrm{Ru(CH_3CN)_2(bpy)_2}]^{2+}$ (1.10 V), ○ $[\mathrm{Ru(NO^{+})(CH_3CN)(bpy)_2}]^{3+}$ (0.19 V), ◆ $[\mathrm{Ru(NO_2)(CH_3CN)(bpy)_2}]^{+}$ (0.81 V).

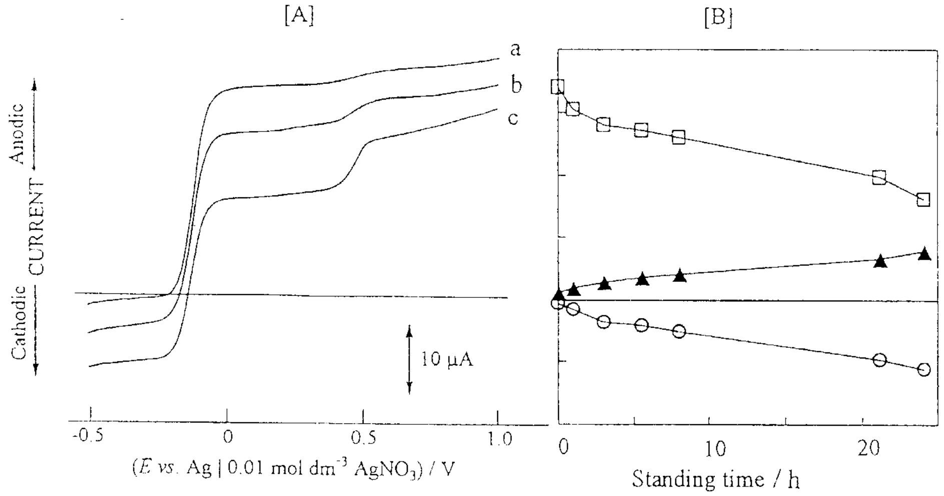

Fig. 5. The conversion process of *cis*-$[\mathrm{Ru(NO^{\bullet})Cl(bpy)_2}]^+$ ($\{\mathrm{RuNO}\}^7$) monitored by hydrodynamic voltammograms (HDV) at 20 °C. [A] Monitoring results. a, Just after the electrolysis was completed (The measurement was carried out after the solution temperature was elevated from −30 to 20 °C); b, 5 h after allowing the electrolyzed solution to stand (Both *cis*-$[\mathrm{RuCl(CH_3CN)(bpy)_2}]^+$ and *cis*-$[\mathrm{Ru(NO^{+})Cl(bpy)_2}]^{2+}$ formed and they increased); c, 24 h after the standing started. [B] Plots of the standing times vs. *I*d values of the product species, each of which was estimated from the corresponding *I*d value of HDV. □*cis*-$[\mathrm{Ru(NO^{\bullet})Cl(bpy)_2}]^+$ (−0.12 V), ▲ *cis*-$[\mathrm{RuCl(CH_3CN)(bpy)_2}]^+$ (0.48 V), ○ *cis*-$[\mathrm{Ru(NO^{+})Cl(bpy)_2}]^{2+}$ (−0.12 V).

$\mathrm{OCOCH_3}$) were formed, and the pattern **ii** type process dominated over the pattern **i-a** type process. It is also noted that the degradation of the pattern **iii** complexes proceeds relatively slowly. The results are shown in Fig. 6A and are summarized graphically in Fig. 6B (in our previous paper[10] we mentioned that *cis*-$[\mathrm{Ru(NO^{\bullet})(OCOCH_3)(bpy)_2}]^+$ does not generate *cis*-$[\mathrm{Ru(NO_2)(CH_3CN)(bpy)_2}]^+$ in any appreciable amount under the conditions; this must be modified as described above, since our experiments when repeated again showed that the formation of the nitro species occurred, although the yield was very low). All electrochemical data of the complexes that relate to the present degradation reactions are summarized in Table 4.

Discussion

Oxygen-Transfer Reactions Occur in *cis*-$[\mathrm{Ru(NO^{\bullet})(ONO_2)(bpy)_2}]^+$ by Two Separate Processes. The complexes *cis*-$[\mathrm{Ru(NO^{\bullet})X(bpy)_2}]^{n+}$ (X = $\mathrm{CH_3CN}$, $\mathrm{H_2O}$, $\mathrm{ONO_2}$), which belong to the pattern **i** group, undergo an oxygen-transfer reaction via a nitrosyl-to-nitro conversion to give identical nitro species *cis*-$[\mathrm{Ru(NO_2)(CH_3CN)(bpy)_2}]^+$; however, reaction sequences of *cis*-$[\mathrm{Ru(NO^{\bullet})(ONO_2)(bpy)_2}]^+$ (pattern **i-b**) definitely differ from those of *cis*-$[\mathrm{Ru(NO^{\bullet})X(bpy)_2}]^{2+}$ (X = $\mathrm{CH_3CN}$, $\mathrm{H_2O}$) (pattern **i-a**); Fig. 3 shows that the formation of *cis*-$[\mathrm{Ru(NO^{\bullet})(CH_3CN)(bpy)_2}]^{2+}$ ($\{\mathrm{RuNO}\}^7$) occurs in *cis*-$[\mathrm{Ru(NO^{\bullet})(ONO_2)(bpy)_2}]^+$ ($\{\mathrm{RuNO}\}^7$) prior to the main reaction of nitrosyl-to-nitro conversion to give *cis*-$[\mathrm{Ru(NO_2)(CH_3CN)(bpy)_2}]^+$. We assume that the elim-

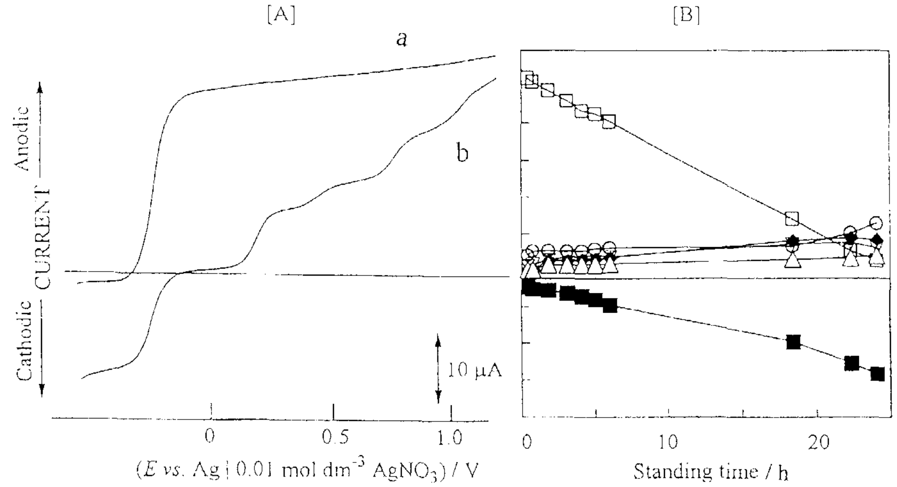

Fig. 6. The conversion process of *cis*-$[Ru(NO^{\bullet})(OCHO)(bpy)_2]^+$ ($\{RuNO\}^7$) monitored by hydrodynamic voltammograms (HDV) at 20 °C. [A] Monitoring results. a, Just after the electrolysis was completed (The measurement was carried out after the solution temperature was elevated from −30 to 20 °C); b, 24 h after the standing started. [B] Plots of the standing times vs. *I*d values of the product species, each of which was estimated from the corresponding *I*d value of HDV. ☐ *cis*-$[Ru(NO^{\bullet})(OCHO)(bpy)_2]^+$ (−0.23 V), ■ *cis*-$[Ru(NO^+)(OCHO)(bpy)_2]^{2+}$ (−0.23 V), ◆ *cis*-$[Ru(NO_2)(CH_3CN)(bpy)_2]^+$ (0.81 V), ○ *cis*-$[Ru(NO^{\bullet})(CH_3CN)(bpy)_2]^{2+}$ (0.19 V), △ *cis*-$[Ru(CH_3CN)_2(bpy)_2]^+$ (1.10 V), ▽ *cis*-$[Ru(OCHO)(CH_3CN)(bpy)_2]^+$ (0.48 V).

Table 4. Electrochemical Data

Complexes	$E^{a)}$/V				
	E_{pc1}	E_{pa1}	$E_{1/2}$ b)	E_{pc2}	ΔE c)
cis-$[Ru(NO)(CH_3CN)(bpy)_2](ClO_4)_3$	0.15	0.23	0.19	−0.71	80
cis-$[Ru(NO)(H_2O)(bpy)_2](ClO_4)_3$	0.09	0.23	0.16	−0.71	160
cis-$[Ru(NO)(ONO_2)(bpy)_2](ClO_4)_2$	−0.10	−0.02	−0.06	−0.77	80
cis-$[Ru(NO)Cl(bpy)_2](ClO_4)_2$	−0.16	−0.08	−0.12	−0.90	80
cis-$[Ru(NO)(OCOCH_3)(bpy)_2](PF_6)_2$	−0.32	−0.22	−0.27	−0.99	100
cis-$[Ru(NO)(OCHO)(bpy)_2](PF_6)_2$	−0.29	−0.19	−0.23	−0.99	100
cis-$[Ru(NO_2)(CH_3CN)(bpy)_2]PF_6$	0.77	0.85	0.81		80
cis-$[Ru(CH_3CN)_2(bpy)_2](PF_6)_2$	1.07	1.13	1.10		60
cis-$[Ru(OCHO)(CH_3CN)(bpy)_2]PF_6$	0.45	0.51	0.48		60
cis-$[RuCl(CH_3CN)(bpy)_2]ClO_4$	0.45	0.52	0.48		70

a) V vs. $Ag|AgNO_3$ (0.1 mol dm^{-3} TEAP–CH_3CN) at 25 °C. b) $(E_{pa1}-E_{pc1})/2$. c) $|E_{pa1}-E_{pc1}|$ (mV). d) *cis*-$[Ru(OCOCH_3)(CH_3CN)(bpy)_2]^+$ ($E_{1/2}$ = 0.42 V) described in the degradation of *cis*-$[Ru(NO^{\bullet})(OCOCH_3)(bpy)_2]^+$ was tentatively identified.

inated NO_3^- ion results in an oxygen-transfer reaction, which brings about the main nitrosyl-to-nitro conversion reaction. A significant difference between *cis*-$[Ru(NO^{\bullet})(ONO_2)(bpy)_2]^+$ and *cis*-$[Ru(NO^{\bullet})X(bpy)_2]^{2+}$ ($X = CH_3CN$, H_2O) is observed in their yield of the nitro species, *cis*-$[Ru(NO_2)(CH_3CN)(bpy)_2]^+$ (yield was calculated as [*I*d of the nitro species]/[*I*d of the original nitrosyl species]×100); nearly 80% of the conversion was achieved in *cis*-$[Ru(NO^{\bullet})(ONO_2)(bpy)_2]^+$, while only 35—40% was estimated for *cis*-$[Ru(NO^{\bullet})X(bpy)_2]^{2+}$ ($X = CH_3CN$, H_2O).

Since the main difference in the conversion process between *cis*-$[Ru(NO^{\bullet})(ONO_2)(bpy)_2]^+$ and *cis*-$[Ru(NO^{\bullet})(CH_3CN)(bpy)_2]^{2+}$ is the presence (or absence) of the nitrate ion in the electrolyzed solution, one may assume that the oxygen source of the nitrosyl-to-nitro conversion will be the nitrate ion released from *cis*-$[Ru(NO^{\bullet})(ONO_2)(bpy)_2]^+$. This assumption was justified by the following experiment. At 20 °C, we added the CH_3CN solution containing Et_4NNO_3 to *cis*-$[Ru(NO^{\bullet})(CH_3CN)(bpy)_2]^{2+}$, which was accumulated by an exhaust reductive electrolysis of *cis*-$[Ru(NO^+)(CH_3CN)(bpy)_2]^{3+}$ at −30 °C. In contrast to the monitoring result observed in *cis*-$[Ru(NO^{\bullet})(CH_3CN)(bpy)_2]^{2+}$ (Fig. 4), the nitro conversion occurred soon, as we have seen in the monitoring experiment of *cis*-$[Ru(NO^{\bullet})(ONO_2)(bpy)_2]^+$ (Fig. 3). Accordingly, the apparent chemical changes of *cis*-$[Ru(NO^+)(ONO_2)(bpy)_2]^{2+}$ to give *cis*-$[Ru(NO_2)(CH_3CN)(bpy)_2]^+$ can be written *formally* by the following equations, if we attempt a simple argument:

$$[Ru(NO^+)(ONO_2)(bpy)_2]^{2+} + e^- \longrightarrow [Ru(NO^{\bullet})(ONO_2)(bpy)_2]^+ \tag{3}$$

$$[Ru(NO^{\bullet})(ONO_2)(bpy)_2]^+ \longrightarrow [Ru(NO^{\bullet})(CH_3CN)(bpy)_2]^{2+} + ONO_2^- \tag{4}$$

$$[\mathrm{Ru(NO^{\bullet})(CH_3CN)(bpy)_2}]^{2+} + \mathrm{ONO_2}^- \longrightarrow [\mathrm{Ru(NO_2)(CH_3CN)(bpy)_2}]^+ + \mathrm{NO_2} \quad (5)$$

That Eq. 5 proceeds, however, is unlikely; Eqs. 3, 4, and 5 can not explain the formation of both *cis*-$[\mathrm{Ru(CH_3CN)_2(bpy)_2}]^{2+}$ and $\{\mathrm{RuNO}\}^6$-type complexes (*cis*-$[\mathrm{Ru(NO^+)(ONO_2)(bpy)_2}]^{2+}$ and *cis*-$[\mathrm{Ru(NO^+)(CH_3CN)(bpy)_2}]^{3+}$), which we detected during the monitoring experiment (see Table 3). As described above, the oxygen source of the nitrosyl-to-nitro conversion observed in *cis*-$[\mathrm{Ru(NO^{\bullet})(ONO_2)(bpy)_2}]^+$ is the nitrate ion released from the complex. We assume that sequences of the reactions described later are proceeding during the conversion reaction; this may explain the generation processes of all the product species which we detected electrochemically in the degradation process of *cis*-$[\mathrm{Ru(NO^{\bullet})(ONO_2)(bpy)_2}]^+$.

We first consider the conversion process of *cis*-$[\mathrm{Ru(NO^{\bullet})(CH_3CN)(bpy)_2}]^{2+}$ (pattern **i-a**), prior to that of *cis*-$[\mathrm{Ru(NO^{\bullet})(ONO_2)(bpy)_2}]^+$ (pattern **i-b**). Undoubtedly, a one-electron reduction of $\{\mathrm{RuNO}\}^6$ complexes occurs at the nitrosyl site.[19] The one-electron reduction species is relatively unstable with respect to elimination of the ($\mathrm{NO^{\bullet}}$) moiety, when the electrolyzed solution is allowed to stand at room temperature. Breaking of the Ru–$\mathrm{NO^{\bullet}}$ bond actually occurred in all complexes investigated here, although the product amount of *cis*-$[\mathrm{Ru(CH_3CN)_2(bpy)_2}]^{2+}$ depends on the X ligand (note also that *cis*-$[\mathrm{Ru(NO^{\bullet})Cl(bpy)_2}]^+$ generates *cis*-$[\mathrm{RuCl(CH_3CN)(bpy)_2}]^+$, instead of *cis*-$[\mathrm{Ru(CH_3CN)_2(bpy)_2}]^{2+}$). Consequently, this elimination leads to the generation of the $\mathrm{NO^{\bullet}}$ moiety (Eq. 6) in addition to *cis*-$[\mathrm{Ru(CH_3CN)_2(bpy)_2}]^{2+}$, which we detected by a monitoring experiment:

$$[\mathrm{Ru(NO^{\bullet})(CH_3CN)(bpy)_2}]^{2+} \longrightarrow [\mathrm{Ru(CH_3CN)_2(bpy)_2}]^{2+} + \mathrm{NO^{\bullet}} \quad (6)$$

The $\mathrm{NO^{\bullet}}$ moiety generated in Eq. 6 results in another reaction, which gives *cis*-$[\mathrm{Ru(NO^+)(CH_3CN)(bpy)_2}]^{3+}$ (Eq. 7), along with the $\mathrm{NO^-}$ moiety, because both $\mathrm{NO^{\bullet}}$ and *cis*-$[\mathrm{Ru(NO^{\bullet})(CH_3CN)(bpy)_2}]^{2+}$ are reactive species owing to their electronic configurations having an unpaired electron.

$$[\mathrm{Ru(NO^{\bullet})(CH_3CN)(bpy)_2}]^{2+} + \mathrm{NO^{\bullet}} \longrightarrow [\mathrm{Ru(NO^+)(CH_3CN)(bpy)_2}]^{3+} + \mathrm{NO^-} \quad (7)$$

Note that *cis*-$[\mathrm{Ru(NO^{\bullet})(CH_3CN)(bpy)_2}]^{2+}$ is available as the most abundant species, at least in the initial stage of the conversion reaction. We emphasize that the sequence of Eq. 7 has actually been established by a separate chemical experiment, described below.

We could find that blowing nitrogen monoxide gas ($\mathrm{NO^{\bullet}}$) into an electrolyzed solution containing *cis*-$[\mathrm{Ru(NO^{\bullet})(CH_3CN)(bpy)_2}]^{2+}$ easily gave the formation of two species, *cis*-$[\mathrm{Ru(NO^+)(CH_3CN)(bpy)_2}]^{3+}$ ($\{\mathrm{RuNO}\}^6$) and *cis*-$[\mathrm{Ru(NO_2)(CH_3CN)(bpy)_2}]^+$, in almost equal quantities, but *cis*-$[\mathrm{Ru(CH_3CN)_2(bpy)_2}]^{2+}$, described in Eq. 6, did not form. Clearly, *cis*-$[\mathrm{Ru(NO_2)(CH_3CN)(bpy)_2}]^+$ (and also *cis*-$[\mathrm{Ru(NO^+)(CH_3CN)(bpy)_2}]^{3+}$) generated in the chemical experiment are formed separately from the electrochemically-induced reaction, in which we have found that *cis*-$[\mathrm{Ru(CH_3CN)_2(bpy)_2}]^{2+}$ is formed, in addition to the $\{\mathrm{RuNO}\}^6$-type complex.

A further reaction, described in Eq. 8, is assumed to occur in the product species of Eq. 7 to give a nitro species, *cis*-$[\mathrm{Ru(NO_2)(CH_3CN)(bpy)_2}]^+$; it has been reported that *cis*-$[\mathrm{Ru(NO^+)(CH_3CN)(bpy)_2}]^{2+}$ behaves as an electrophile,[19,20] and that the $\mathrm{NO^-}$ moiety as a two-electron reduction species of $\mathrm{NO^+}$ would be reactive toward electrophiles. Presently, however, a detailed mechanistic process of how the $\mathrm{NO^-}$ moiety behaves in the nitrosyl-to-nitro conversion is difficult to explain, and the evolution of $\mathrm{N_2O}$ in Eq. 8 has not yet been confirmed.

$$[\mathrm{Ru(NO^+)(CH_3CN)(bpy)_2}]^{3+} + 2\mathrm{NO^-} \longrightarrow [\mathrm{Ru(NO_2)(CH_3CN)(bpy)_2}]^+ + \mathrm{N_2O} \quad (8)$$

In the degradation of *cis*-$[\mathrm{Ru(NO^{\bullet})(ONO_2)(bpy)_2}]^+$ (pattern **i-b**), two separate nitrosyl-to-nitro conversion processes exist. Since elimination of the $\mathrm{ONO_2}^-$ moiety occurs easily (see Fig. 3B), essentially the same reaction as that described in *cis*-$[\mathrm{Ru(NO^{\bullet})(CH_3CN)(bpy)_2}]^{2+}$ (Eqs. 6, 7, and 8) proceeds initially; this leads to the formation of *cis*-$[\mathrm{Ru(NO_2)(CH_3CN)(bpy)^2}]^+$, along with *cis*-$[\mathrm{Ru(NO^+)(CH_3CN)(bpy)_2}]^{3+}$ and *cis*-$[\mathrm{Ru(CH_3CN)_2(bpy)_2}]^{2+}$, including a small amount of *cis*-$[\mathrm{Ru(NO^+)(ONO_2)(bpy)_2}]^{2+}$, whose formation is explained by.

$$[\mathrm{Ru(NO^{\bullet})(ONO_2)(bpy)_2}]^+ + \mathrm{NO^{\bullet}} \longrightarrow [\mathrm{Ru(NO^+)(ONO_2)(bpy)_2}]^{2+} + \mathrm{NO^-} \quad (9)$$

Another reaction which affords effectively *cis*-$[\mathrm{Ru(NO_2)(CH_3CN)(bpy)_2}]^+$ follows in the second stage of the degradation reaction of *cis*-$[\mathrm{Ru(NO^{\bullet})(ONO_2)(bpy)_2}]^+$. Figure 3 shows that a large amount of the nitro species is generated after liberation of the $\mathrm{ONO_2}^-$ ligand to give *cis*-$[\mathrm{Ru(NO^{\bullet})(CH_3CN)(bpy)_2}]^{2+}$ is almost completed; the result is explainable if the liberated $\mathrm{ONO_2}^-$ participates in the oxygen-transfer reaction. Although the mechanistic process is not clear again, we believe that the $\mathrm{NO_3}^-$ is able to react with the $\mathrm{NO^-}$. However, such chemistry concerning the $\mathrm{NO_3}^-$ and $\mathrm{NO^-}$ moieties in solution, involving a one-electron reduction nitrosyl species, is beyond the limits of our electrochemical investigation. We concluded that the pattern **i-b** reaction involves two types of nitrosyl-to-nitro conversion reactions; an initial conversion proceeds by the same mechanistic process as that described in the pattern **i-a** reaction, although the yield of the nitro species is very low. The main conversion due to the released $\mathrm{ONO_2}^-$ occurs in the second stage of the degradation reaction in *cis*-$[\mathrm{Ru(NO^{\bullet})(ONO_2)(bpy)_2}]^+$ (Fig. 3B).

No Oxygen Transfer Reaction Occurs in *cis*-$[\mathrm{Ru(NO^{\bullet})Cl(bpy)_2}]^+$, in Which a Precursor Species (*cis*-$[\mathrm{Ru(NO^{\bullet})(CH_3CN)(bpy)_2}]^{2+}$) Is Not Formed. The formation of *cis*-$[\mathrm{Ru(NO^{\bullet})(CH_3CN)(bpy)_2}]^{2+}$ ($\{\mathrm{RuNO}\}^7$) must be a key procedure for the oxygen-transfer reaction, either in pattern **i-a** or in pattern **i-b**. The monitoring results of *cis*-$[\mathrm{Ru(NO^{\bullet})Cl}$-

(bpy)$_2$]$^+$ ($\{$RuNO$\}^7$, pattern **ii**) strongly support this assumption. We detected only two species, *cis*-[RuCl(CH$_3$CN)(bpy)$_2$]$^+$ and *cis*-[Ru(NO$^+$)Cl(bpy)$_2$]$^{2+}$ ($\{$RuNO$\}^6$), as the degradation products (Fig. 5), which might be explained by Eqs. 10 and 11. Neither *cis*-[Ru(NO$^\bullet$)(CH$_3$CN)(bpy)$_2$]$^{2+}$ nor *cis*-[Ru(NO$_2$)(CH$_3$CN)(bpy)$_2$]$^+$ was observed to form in this degradation. Throughout a monitoring study of *cis*-[Ru(NO$^\bullet$)Cl(bpy)$_2$]$^+$, we could confirm the absence of *cis*-[Ru(NO$^\bullet$)(CH$_3$CN)(bpy)$_2$]$^{2+}$, which we assumed to be the precursor of *cis*-[Ru(NO$_2$)(CH$_3$CN)(bpy)$_2$]$^+$.

$$[\mathrm{Ru(NO^\bullet)Cl(bpy)_2}]^+ \longrightarrow [\mathrm{RuCl(CH_3CN)(bpy)_2}]^+ + \mathrm{NO^\bullet} \quad (10)$$

$$[\mathrm{Ru(NO^\bullet)Cl(bpy)_2}]^+ + \mathrm{NO^\bullet} \longrightarrow [\mathrm{Ru(NO^+)Cl(bpy)_2}]^{2+} + \mathrm{NO^-} \quad (11)$$

A previous investigation showed that, in CH$_3$CN, the solvation of the aqua ligand in *cis*-[Ru(NO$^+$)(H$_2$O)(bpy)$_2$]$^{3+}$ ($\{$RuNO$\}^6$) is relatively inert,[10] but that of the corresponding *cis*-[Ru(NO$^\bullet$)(H$_2$O)(bpy)$_2$]$^{2+}$ ($\{$RuNO$\}^7$) proceeds rapidly. Such a solvation, which gives *cis*-[Ru(NO$^\bullet$)(CH$_3$CN)(bpy)$_2$]$^{2+}$, does not occur in *cis*-[Ru(NO$^\bullet$)Cl(bpy)$_2$]$^+$ (pattern **ii**).

In pattern **iii**, *cis*-[Ru(NO$^\bullet$)X(bpy)$_2$]$^+$ (X = HCOO, CH$_3$COO, NO$_2$) gave many reaction products, without any major product species. We believe that the result stems from the chemical reactivity of *cis*-[Ru(NO$^\bullet$)X(bpy)$_2$]$^{n+}$ (X = HCOO, CH$_3$COO, NO$_2$), which brings about two types of degradation reactions, the patterns **i-a** and **ii**; although the ligand substitution which gives *cis*-[Ru(NO$^\bullet$)(CH$_3$CN)(bpy)$_2$]$^{2+}$ occurs in *cis*-[Ru(NO$^\bullet$)X(bpy)$_2$]$^{n+}$ (X = HCOO and CH$_3$COO for $n = 1$), it proceeds very slowly (see Fig. 6). The substitution inertness results in the formation of small amounts of three product species (*cis*-[Ru(NO$_2$)(CH$_3$CN)(bpy)$_2$]$^+$, *cis*-[Ru(NO$^\bullet$)(CH$_3$CN)(bpy)$_2$]$^{2+}$, and *cis*-[Ru(CH$_3$CN)$_2$(bpy)$_2$]$^{2+}$), through the pattern **i-a** reaction. In addition, *cis*-[Ru(NO$^\bullet$)X(bpy)$_2$]$^+$ (X = HCOO and CH$_3$COO) underwent bonding rupture in the (Ru–NO$^\bullet$) moiety to give *cis*-[RuX(CH$_3$CN)(bpy)$_2$]$^+$; this is a similar pattern to the one we have seen in the degradation process of *cis*-[Ru(NO$^\bullet$)Cl(bpy)$_2$]$^+$ (pattern **ii**). We concluded that the present nitrosyl-to-nitro conversion occurred depending on the lability of the X ligand in *cis*-[Ru(NO$^\bullet$)X(bpy)$_2$]$^{n+}$, which gave *cis*-[Ru(NO$^\bullet$)(CH$_3$CN)(bpy)$_2$]$^{n+}$.

A question arose as to why the NO$^-$ moiety did not react with *cis*-[Ru(NO$^+$)(ONO$_2$)(bpy)$_2$]$^{2+}$ (Eq. 9) (and also with *cis*-[Ru(NO$^+$)Cl(bpy)$_2$]$^{2+}$ (Eq. 11)), although *cis*-[Ru(NO$^\bullet$)(CH$_3$CN)(bpy)$_2$]$^{2+}$ (Eq. 8) did react well. It has been reported that the nitrosyl reactivity of $\{$RuNO$\}^6$-type complexes depends strongly on the nature of the co-existing ligand X; the criterion due to ν (NO) data[20] shows that *cis*-[Ru(NO$^+$)(CH$_3$CN)(bpy)$_2$]$^{3+}$ ($\{$RuNO$\}^6$) is rather more reactive than *cis*-[Ru(NO$^+$)Cl(bpy)$_2$)]$^{2+}$ ($\{$RuNO$\}^6$).[19] In this context, we recall a result similar to that observed here, which has been reported previously;[21] we found that *cis*-[Ru(NO$^+$)(CH$_3$CN)(bpy)$_2$]$^{3+}$ reacted with even a free NO$_2{}^-$ ion to give a small amount of *cis*-[Ru(NO$_2$)(CH$_3$CN)(bpy)$_2$]$^+$,[21] although the corresponding *cis*-[Ru(NO$^+$)Cl(bpy)$_2$]$^{2+}$ did not afford the nitro species. It appears that *cis*-[Ru(NO$^+$)(CH$_3$CN)(bpy)$_2$]$^{3+}$ has an exceptional electrophilicity toward nucleophiles.

Additional Results Concerning the Present Observations. A previous study has reported that the one-electron reduction species *cis*-[Ru(NO$^\bullet$)Cl(bpy)$_2$]$^+$ is quite chemi-

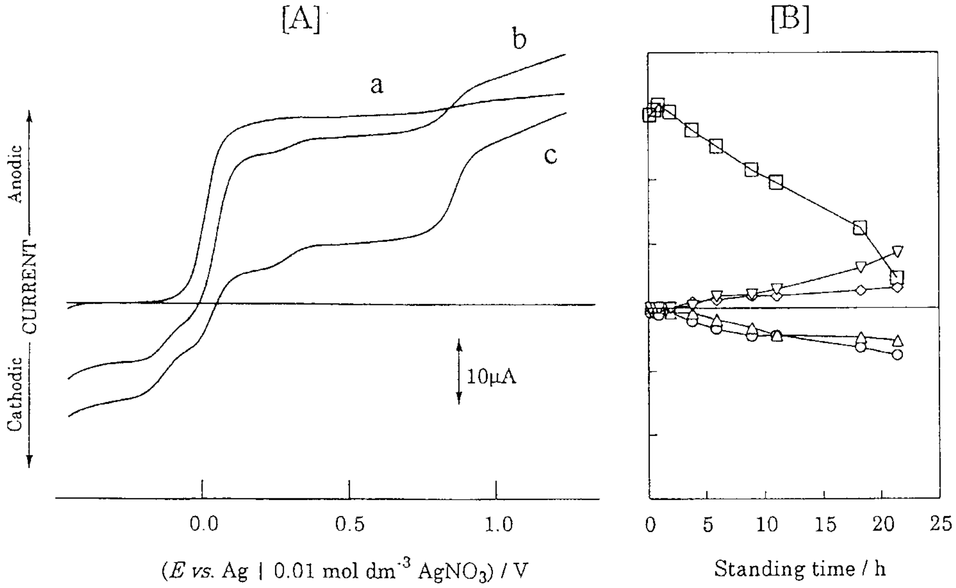

Fig. 7. The conversion process of *cis*-[Ru(NO$^\bullet$)(NO$_2$)(bpy)$_2$]$^+$ ($\{$RuNO$\}^7$) monitored by hydrodynamic voltammograms (HDV) at 20 °C. [A] Monitoring results. a, Just after the electrolysis was completed (The measurement was carried out after the solution temperature was elevated from -30 to 20 °C); b, 11 h after allowing the electrolyzed solution to stand; c, 24 h after the standing started. [B] Plots of the standing times vs. *I*d values of the products species, each of which was estimated from the corresponding *I*d value of HDV. □ *cis*-[Ru(NO$^\bullet$)(NO$_2$)(bpy)$_2$]$^+$ (-0.03 V), ▼ *cis*-[Ru(NO$_2$)(CH$_3$CN)(bpy)$_2$]$^+$ (0.81 V), ◇ *cis*-[Ru(NO$^\bullet$)(CH$_3$CN)(bpy)$_2$]$^+$ (0.19 V), ○ *cis*-[Ru(NO$^+$)(NO$_2$)(bpy)$_2$]$^{2+}$ (-0.03 V), △ *cis*-[Ru(NO)(ONO)(bpy)$_2$]$^{2+}$ (-0.19 V).

cally stable, at least within the time scale of an electrolysis, while the corresponding trans isomer is unstable.[22] We attempted to monitor the degradation reaction of *trans*-$[Ru(NO^{\bullet})Cl(bpy)_2]^+$. However, the result is difficult to explain, because many species were formed as degradation products that have been difficult to characterize so far.

Our recent study has also shown that *cis*-$[Ru(NO^+)(ONO)(bpy)_2]^{2+}$ undergoes a facile structural rearrangement to give the corresponding nitro isomer, *cis*-$[Ru(NO^{\bullet})(NO_2)(bpy)_2]^+$, when the nitrito isomer undergoes a one-electron reduction.[12] The resultant nitro species can be returned to the original nitrito species by a one-electron oxidation. We did not investigate the further behavior of *cis*-$[Ru(NO^{\bullet})(NO_2)(bpy)_2]^+$, whether it shows the nitrosyl-to-nitro conversion or not,[12] so we attempted the monitoring study described above using *cis*-$[Ru(NO^{\bullet})(NO_2)(bpy)_2]^+$. Figures 7A and 7B show that basically the same degradation as that observed in the pattern **iii** occurred; three species (*cis*-$[Ru(NO^{\bullet})(CH_3CN)(bpy)_2]^{2+}$, *cis*-$[Ru(NO_2)(CH_3CN)(bpy)_2]^+$, and *cis*-$[Ru(NO^+)(NO_2)(bpy)_2]^{2+}$) were detected to form, each in small scale, along with *cis*-$[Ru(NO^+)(ONO)(bpy)_2]^{2+}$. The nitrogen atom of *cis*-$[Ru(NO_2)(CH_3CN)(bpy)_2]^+$ may come from either nitrosyl or nitro nitrogen, since either the pattern **i-a** type degradation or the pattern **ii** type degradation is operating.

It is well known that the ClO_4^- ion is potentially a strong oxidant. Despite the possibility that it participates in the present oxidative reactions, we found that the experiment carried out under conditions containing large amounts of ClO_4^- ion did not accelerate the nitrosyl-to-nitro conversion. We observed that *cis*-$[Ru(NO^+)(CH_3CN)(bpy)_2]^{3+}$ (ClO_4 salt was used) was converted to give *cis*-$[Ru(NO_2)(CH_3CN)(bpy)_2]^+$, as mentioned earlier, in a nearly 40% yield in maximum, when $(R_4N)ClO_4$ was added as a supporting electrolyte. We tried the experiment using *cis*-$[Ru(NO^+)(CH_3CN)(bpy)_2](PF_6)_3$, with $(R_4N)PF_6$ as a supporting electrolyte, but the extent of the conversion was almost the same in both cases.

Unlike *cis*-$[Ru(NO^{\bullet})X(bpy)_2]^{n+}$-type complexes, *cis*-$[Ru(NO^{\bullet})X(bpy)(py)_2]^{n+}$ type complexes (X = OCOMe, NO_2)[23] show gradual pyridine ligand elimination, along with the pattern **ii**-type degradation reaction. In *cis*-$[Ru(NO^{\bullet})(NH_3)(bpy)(py)_2]^{n+}$, however, the HDV and CV voltammograms of the species were maintained without any marked chemical changes, at least for 10 h; this suggests that the present monitoring experiments were carried out under careful conditions and were sufficiently protected from air oxidation, although the $\{RuNO\}^7$-type complexes investigated here are all air-sensitive species.

Let us cite a few recent brief comments on the electrochemically-induced nitrosyl-to-nitro conversion. Meyer and his coworkers have reported that an electrochemical reduction of *cis*-$[Ru(NO^+)(CH_3CN)(bpy)_2]^{3+}$ might afford *cis*-$[Ru(NO_2)(CH_3CN)(bpy)_2]^+$, along with some other unidentified material,[8] as mentioned earlier. They have also reported that the reduction of $[Ru(NO^+)(terpy)(acac)]^{2+}$ gave the corresponding nitro species, although product identification was not established.[9] Interestingly, their nitrosyl-to-nitro conversions were found in exhaust reductive electrolyses carried out at the *second reduction potential* of the nitrosyl complexes, although the present conversion proceeded in the electrolyses at the *first reduction potential*. Our recent study has shown that the nitrosyl-to-nitro conversion occurred when a binuclear complex having a two-electron reduction nitrosyl ($[Ru_2(NO^-)_2(bpy)_4]^{2+}$ ($\{RuNO\}^8-\{RuNO\}^8$)) was disintegrated at room temperature in CH_3CN.[10] Electrochemical monitoring of the conversion reaction indicated that the μ_2-nitrosyl binuclear complex gave *cis*-$[Ru(NO^{\bullet})(CH_3CN)(bpy)_2]^{2+}$ as an initial degradation product.

This work was supported by a Grant-in-Aid for Scientific Research No.09640622 from the Ministry of Education, Science, Sports and Culture.

References

1 Nitrosyl complexes with formal oxidation state of $(Ru^{II}NO^+)$ are abbreviated as $\{RuNO\}^6$: J. Enemark and R. D. Feltham, *Coord. Chem. Rev.*, **13**, 339 (1974).

2 M. N. Hughes, "The Inorganic Chemistry of Biological Processes," 2nd ed, John Wiley & Sons, New York (1981).

3 G. B. Richter-Addo and P. Legdzins, "Metal Nitrosyls," Oxford Univ. Press, New York (1992).

4 J. H. Swinehart, *Coord. Chem. Rev.*, **2**, 385 (1967).

5 F. Bottomley, *Acc. Chem. Res.*, **11**, 158 (1978).

6 J. A. McCleverty, *Chem. Rev.*, **79**, 53 (1979).

7 F. Bottomley, *React. Coord. Ligands*, **2**, 115 (1989).

8 R. W. Callahan and T. J. Meyer, *Inorg. Chem.*, **16**, 574 (1977).

9 A. Dovletoglou, S. A. Adeymi, and T. J. Meyer, *Inorg. Chem.*, **35**, 4120 (1996).

10 H. Nagao, N. Nagao, Y. Yukawa, D. Ooyama, Y. Sato, T. Oosawa, H. Kuroda, F. S. Howell, and M. Mukaida, *Bull. Chem. Soc. Jpn.*, **72**, 1273 (1999).

11 T. J. Meyer and J. B. Godwin, *Inorg. Chem.*, **10**, 471 (1971). In their reference, *cis*-$[RuCl_2(bpy)_2]$ has been used as a starting material of the synthesis. Instead, we used *cis*-$[RuCl_2(bpy)_2]Cl$, because the complex is available in relatively high yield and in convenient form (Ref. 14).

12 D. Ooyama, N. Nagao, H. Nagao, Y. Miura, A. Hasegawa, K. Ando, F. S. Howell, M. Mukaida, and K. Tanaka, *Inorg. Chem.*, **34**, 6024 (1995).

13 D. Ooyama, H. Nagao, K. Ito, N. Nagao, Y. Miura, F. S. Howell, and M. Mukaida, *Bull. Chem. Soc. Jpn.*, **70**, 2141 (1997).

14 F. Bottomley and M. Mukaida, *Inorg. Chim. Acta*, **L29** (1985).

15 K. Nakamoto, "Infrared and Raman Spectra of Inorganic and Coordination Compounds," 3rd ed, John Wiley and Sons, New York (1978).

16 H. Nagao, D. Ooyama, F. S. Howell, M. Mukaida, and K. Mizumachi, *Anal. Sci.*, **14**, 645 (1998).

17 The nitrosyl-to-nitro conversion in these complexes has been described partly in Ref. 10. The extended investigation is described here, because the degradations of both *cis*-$[Ru(NO^{\bullet})(CH_3CN)(bpy)_2]^+$ and *cis*-$[Ru(NO^{\bullet})(H_2O)(bpy)_2]^+$ are necessary for our present argument, along with that of *cis*-$[Ru(NO^{\bullet})(ONO_2)(bpy)_2]^+$.

18 N. Nagao, D. Ooyama, K. Oomura, Y. Miura, F. S. Howell, and M. Mukaida, *Inorg. Chim. Acta*, **225**, 111 (1994).

19 R. W. Callahan and T. J. Meyer, *Inorg. Chem.*, **21**, 574

(1977).

20 F. Bottomley, *J. Chem. Soc., Chem. Commun.*, **1973**, 919.

21 H. Nagao, K. Ito, N. Tsuboya, D. Ooyama, N. Nagao, F. S. Howell, and M. Mukaida, *Inorg. Chim. Acta*, **290**, 113 (1999).

22 H. Nagao, H. Nishimura, H. Funato, Y. Ichikawa, F. S. Howell, M. Mukaida, and H. Kakihana, *Inorg. Chem.*, **28**, 3955 (1989).

23 Such complexes have been synthesized as previously reported: D. Ooyama, Y. Miura, Y. Kanazawa (Kitanaka), F. S. Howell, N. Nagao, M. Mukaida, H. Nagao, and K. Tanaka, *Inorg. Chim. Acta*, **237**, 47 (1995).